



Published in final edited form as:

J Control Release. 2008 December 18; 132(3): 193–199. doi:10.1016/j.jconrel.2008.07.014.

Tumor-Targeted HPMA Copolymer-(RGDfK)-(CHX-A"-DTPA) Conjugates Show Increased Kidney Accumulation

Mark P. Borgman^{1,2}, Tomika Coleman³, Rohit B. Kolhatkar^{1,2}, Sandra Geyser-Stoops³, Bruce R. Line^{2,3,4,†}, and Hamidreza Ghandehari^{1,2,4,*}

¹Department of Pharmaceutical Sciences, University of Maryland, Baltimore, Maryland-21201, USA

²Center for Nanomedicine and Cellular Delivery, University of Maryland, Baltimore, Maryland-21201, USA

³Division of Nuclear Medicine, Department of Radiology, University of Maryland, Baltimore, Maryland-21201, USA

⁴Greenebaum Cancer Center, University of Maryland, Baltimore, Maryland-21201, USA

Abstract

N-(2-hydroxypropyl) methacrylamide (HPMA) copolymer-RGDfK conjugates targeting the $\alpha_v\beta_3$ integrin have shown increased accumulation in solid tumors and promise for selective delivery of radiotherapeutics to sites of angiogenesis- or tumor-expressed $\alpha_v\beta_3$ integrin. An unresolved issue in targeting radiotherapeutics to solid tumors is toxicity to non-target organs. To reduce toxicity of radiolabeled conjugates, we have synthesized HPMA copolymer-RGDfK conjugates with varying molecular weight and charge content to help identify a polymeric structure that maximizes tumor accumulation while rapidly clearing from non-targeted organs. Endothelial cell binding studies showed that copolymer conjugates of approximately 43, 20 and 10 kD actively bind to the $\alpha_v\beta_3$ integrin. Scintigraphic images showed rapid clearance of indium-111 radiolabeled conjugates from the blood pool and high kidney accumulation within 1 h in tumor bearing mice. Biodistribution data confirms images with high accumulation in kidney (max 210% ID/g for 43 kD conjugate) and lower tumor accumulation (max 1.8% ID/g for 43kD conjugate). While actively binding to the $\alpha_v\beta_3$ integrin in vitro, HPMA copolymer-RGDfK conjugates with increased negative charge through increased CHX-A"-DTPA chelator content in the side chains causes increased kidney accumulation with a loss of tumor binding in vivo.

Keywords

HPMA Copolymer; RGD; Biodistribution; Tumor targeting; Renal targeting

© 2008 Elsevier Inc. All rights reserved.

*Corresponding author present address: Hamidreza Ghandehari, PhD, Departments of Pharmaceutics & Pharmaceutical Chemistry and Bioengineering, University of Utah, 383 Colorow Road, Room 343, Salt Lake City, Utah-84108, Tel: (801) 587-1566, Email: E-mail: hamid.ghandehari@pharm.utah.edu.

†Deceased

Dedicated to our mentor, colleague and friend Dr. Bruce Line

Publisher's Disclaimer: This is a PDF file of an unedited manuscript that has been accepted for publication. As a service to our customers we are providing this early version of the manuscript. The manuscript will undergo copyediting, typesetting, and review of the resulting proof before it is published in its final citable form. Please note that during the production process errors may be discovered which could affect the content, and all legal disclaimers that apply to the journal pertain.

INTRODUCTION

As therapy effectors, radioisotopes have advantages over chemotherapeutics because they can kill cells over a range of distances from the site of localization, providing a strategy to address cancer cell clonal diversity and tumor microenvironmental heterogeneity [1]. The $\alpha_v\beta_3$ integrin provides a target that is broadly expressed in tumors greater than 1 mm related to angiogenesis, tumor associated macrophages and to tumor cell expression [2–4]. *N*-(2-hydroxypropyl) methacrylamide (HPMA) copolymers were developed with attached cyclized Arg-Gly-Asp (RGD) motifs that preferentially target the $\alpha_v\beta_3$ integrin over-expressed in tumors [5–7]. HPMA copolymers with cyclized RGD sequences in the side chains showed enhanced tumor accumulation over non-targeted copolymers. Additionally, polymers radiolabeled with the beta-emitting radionuclide yttrium-90 exhibited potential for targeted radiotherapy by causing tumor growth delay [8]. However, it is necessary to further develop systems that minimize non-tumor accumulation to decrease adverse effects of radiation.

To develop an efficacious molecularly guided radiotherapeutic it is necessary to construct a delivery system that provides a high therapeutic index [9]. One way to improve the therapeutic index of HPMA copolymers is by controlling the size and charge of the polymeric carrier. It was shown that lower molecular weight and the added presence of electronegative charge increased the rate of elimination of such copolymers and decreased organ accumulation [10–13]. Smaller molecular weight polymers tend to accumulate less in tumor tissue, however when comparing relative levels of tumor-to-organ accumulation little difference has been demonstrated [10]. Such studies however have not been systematically carried out with HPMA copolymers that actively target the tumor.

In order to evaluate the effects of molecular weight and charge of HPMA copolymer-cyclic-RGD conjugates on tumor targeting and organ localization we have synthesized targetable copolymers with higher negative charge content and varying molecular weight. The current work reports synthesis, characterization, in vitro cell-binding and in vivo biodistribution of three HPMA copolymer-RGDfK conjugates in tumor-bearing mice.

METHODS

Chemicals

RGDfK (MW 604.5) was obtained from AnaSpec Inc. (San Jose, CA). *N*-[(*R*)-2-Amino-3-(*p*-isothiocyanatophenyl)propyl]-*trans*-(*S,S*)-cyclohexane-1,2-diamine-*N,N,N',N'',N'''*-pentaacetic acid (*p*-SCN-CHX-A''-DTPA) was obtained from Macrocylics (Dallas, TX) and *N*-(3-Aminopropyl)methacrylamide hydrochloride (APMA) from Polysciences Inc. (Warrington, PA). ^{125}I -echistatin (2000 Ci/mmol) was purchased from GE Healthcare (Piscataway, NJ). Indium-111 was obtained as $^{111}\text{InCl}_3$ from Mallinckrodt Inc. (Beltsville, MD) in 0.05M HCl. All amino acids used were of *L*-configuration. All other chemicals were of reagent grade as obtained from Sigma Chemical Co. (St. Louis, MO).

Synthesis and characterization of comonomers

N-(2-hydroxypropyl) methacrylamide (HPMA) (m.p. 66–68 °C, MW 143.8) [14]; reactive ester comonomer, *N*-methacryloylglycylglycyl-*p*-nitrophenyl ester (MA-GG-ONp) ($\epsilon_{273} = 9280.7 \text{ M}^{-1}\text{cm}^{-1}$, m.p. 160–163 °C, MW 321.7) [15]; and ^{111}In chelating comonomer, *N*-methacryloylaminopropyl-2-amino-3-(isothiourea-phenyl) propyl-cyclohexane-1,2-diamine-*N,N,N',N'',N'''*-pentaacetic acid (APMA-CHX-A''-DTPA) ($\epsilon_{274} = 5114.6 \text{ M}^{-1}\text{cm}^{-1}$, MW 736.7) [8] were synthesized and characterized according to previously described methods. *N*-methacryloylglycylglycyl-RGDfK (MA-GG-RGDfK, MW 786.9) was synthesized via *p*-nitrophenyl ester aminolysis of MA-GG-ONp in dry DMF in the presence of pyridine for 48h.

Pure product was obtained by preparatory HPLC (Varian Prostar, Palo Alto, CA) with a Microsorb 100 C-18 reversed phase column 250×10 mm using a gradient mixture of water with 0.1% trifluoroacetic acid (TFA) and acetonitrile with 0.1% TFA at 2ml/min. The product was monitored by UV spectrophotometry ($\lambda=220$), and elution peaks pooled and lyophilized.

Synthesis and characterization of HPMA copolymer-RGDfK conjugates

HPMA copolymers were synthesized via free radical precipitation copolymerization of comonomers in 100% dimethyl sulfoxide (DMSO) using *N, N'*-azobisisobutyronitrile (AIBN) as the initiator [14] and 15 mol% (of total monomer feed) 3-mercaptopropionic acid (MPA) as a chain transfer agent [16]. The feed composition of the comonomers was 10 mol% for MA-GG-RGDfK, 10 mol% for APMA-CHX-A''-DTPA, and 80 mol% for HPMA. The comonomer mixtures were sealed in an ampoule under nitrogen and stirred at 50 °C for 24 h. Afterwards, DMSO was removed by rotary evaporation. The copolymer precipitate was dissolved in and dialyzed (MWCO=3500) against deionized water for 48 h followed by lyophilization. Copolymers of varying molecular weight were obtained by size-exclusion fractionation on a Superose 12 preparative column (16mm × 50cm) (GE Healthcare) using a Fast Protein Liquid Chromatography (FPLC) system (GE Healthcare). Respective fractions were pooled, desalted over a Sephadex G-25 (PD-10) column, and lyophilized from deionized water.

The peptide content in the conjugates was determined by amino acid analysis (Commonwealth Biotechnologies, Richmond, VA). CHX-A''-DTPA content was determined by UV spectrophotometric analysis of copolymer products ($\lambda=274$ nm) using a standard calibration curve of CHX-A''-DTPA in 100% DMSO. Weight average molecular weight (M_w) and polydispersity (M_w/M_n) were estimated by size exclusion chromatography (SEC) on a Superose 12 column (10 mm × 30 cm) (GE Healthcare, Piscataway, NJ) with fractions of known molecular weight HPMA copolymers using FPLC.

Cell lines

Mouse Lewis lung carcinoma cells (LLC1: ATCC, Manassas, VA) were cultured in DMEM (Life Technologies Inc., Grand Island, NY) supplemented with 4 mM L-glutamine, 10% (v/v) heated-inactivated fetal bovine serum (FBS), 4.5g/L glucose and 1.5g/L sodium bicarbonate at 37 °C in a humidified atmosphere of 5% CO₂ (v/v). HUVECs [17] were cultured in endothelial cell growth media-2 (EGM-2: Lonza, Walkersville, MD) at 37 °C in a humidified atmosphere of 5% CO₂ (v/v). For all experimental procedures, confluent cells, in 24 h culture without media change, were harvested with 0.05% trypsin/0.02% EDTA in PBS.

Mouse model of Lewis lung carcinoma

Lewis lung carcinoma (LLC1) cells were collected, washed, counted and resuspended in DMEM. 5×10^5 cells (50 μ l) mixed with 50 μ l Matrigel (Becton Dickinson Biosciences, Bedford, MA) were injected subcutaneously in the right front subaxillary zone of each female Taconic C57BL/6 mouse (6–8 weeks old, 20–25 g). During experiments the animals were sedated with an intraperitoneal injection of pentobarbital (50mg/kg body weight) and studied under an approved protocol of the University of Maryland Baltimore Institutional Animal Care and Use Committee (IACUC).

Cell receptor binding assay

The binding affinities of free RGDfK peptide and HPMA copolymer-RGDfK conjugates were assessed using a competitive binding assay to the $\alpha_v\beta_3$ integrin expressed on HUVECs with ¹²⁵I-echistatin [18,19]. HUVECs were harvested, washed with PBS, resuspended in binding buffer (20 mmol/L Tris, pH 7.4, 150 mmol/L NaCl, 2 mmol/L CaCl₂, 1 mmol/L MgCl₂, 1 mmol/L MnCl₂, 0.1% bovine serum albumin) and seeded in 96-well Multiscreen HV

filter plates (0.45 μm ; Millipore) at 50,000 cells per well. Cells were co-incubated at 4°C for 2 h with ^{125}I -echistatin (0.05 nM) and increasing peptide equivalent concentrations of polymers or free RGDfK (0–100 μM), and final volume adjusted to 200 μL all in binding buffer. Following incubation, the plates were filtered using a Multiscreen vacuum manifold (Millipore, Billerica, MA) and washed twice with cold binding buffer. Filters were harvested and radioactivity determined by γ -counting (Perkin Elmer Wizard, 1470 Automatic Gamma Counter) to determine percent bound ^{125}I -echistatin. Nonspecific binding was determined by incubating cells with a 200-fold excess of cold echistatin. Nonlinear regression analysis and determination of IC_{50} values was performed using GraphPad Prism (GraphPad Software, Inc.). Each data point represents the average of triplicate wells.

^{111}In radiolabeling of conjugates

The polymer conjugates were labeled by chelating ^{111}In to CHX-A"-DTPA in the side-chains using a slight modification of a method previously described [20]. Briefly, the hydrochloride solution (0.5 mL) of ^{111}In was buffered to approximately pH 5.0 with 100 μl of 1 M sodium acetate buffer to which 2 mg of copolymer conjugate in 100 μl of sodium acetate buffer was added, followed by incubation at 50 °C for 45 min (pH 5.0) in an evacuated sterile vial. The reaction was quenched with 50 μl of 0.05 M EDTA over 10 min at 22 °C to scavenge any free ^{111}In . The labeled conjugates were isolated in normal saline over a Sephadex G-25 (PD-10) column.

Imaging and biodistribution studies

Animals were injected via the lateral tail vein with 100 μl of normal saline containing 12 nmol peptide equivalent (1.3–4.1 nmol polymer) of each ^{111}In labeled HPMA copolymer-RGDfK conjugate (136–230 μCi) per mouse. Sequential 1-min scintigraphic images were obtained for 30-min at 1, 24, 48, and 96 h post-intravenous injection using a DSX-LI dual head gamma camera with a low energy all-purpose collimator (SMV, Twinsburg, OH).

Time dependent biodistribution studies were carried out by sacrificing mice at 15 min, 1, 6, 24, 48, 96, 192, and 240 h post-injection (p.i.). At the time of euthanasia, blood samples were collected by cardiac puncture. During necropsy, whole organ tissue samples were obtained from the heart, lung, liver, spleen, kidney, small intestine, large intestine, stomach, muscle, tumor, and tail. The tissue samples were washed with water, counted (Perkin Elmer Wizard, 1470 Automatic Gamma Counter), weighed and the percentage-injected dose per gram tissue (%ID/g) was calculated. In addition, urine and feces were collected from a cohort of 4 animals per treatment group using metabolic cages (Techniplast, Exton, PA) and radioactivity measured until no additional dose was recovered (72 h p.i.). All biodistribution studies were performed with three or four mice per group.

Statistical Analysis

Differences in organ accumulation and urinary excretion of the copolymer conjugates were analyzed using one-way ANOVA. Where differences were detected, Tukey's test was used to test for pairwise differences between the groups.

RESULTS

Physicochemical characteristics of HPMA copolymer-RGDfK conjugates

The characteristics of HPMA copolymer-RGDfK conjugates are reported in Table 1. Copolymers of approximately 43, 20 and 10 kD were obtained with low polydispersity via size fractionation. SEC profiles (not shown) indicated the absence of small molecular weight impurities. Copolymers of increased negative charge were synthesized by incorporating a 10

mol% APMA-CHX-A"-DTPA feed ratio, containing approximately 11, 5 and 3 CHX-A"-DTPA units per backbone, respectively. The charge content as estimated by UV absorbance for CHX-A"-DTPA was 1.3–1.4 mmol carboxylic acid group per g polymer for the conjugates. The conjugates contained about 9, 6 and 3 RGDfK units per polymer backbone respectively, as determined by size exclusion chromatography and amino acid analysis. Specific activities of 0.13 mCi/nmol (3.0 mCi/mg polymer), 0.07 mCi/nmol (3.5 mCi/mg polymer) and 0.03 mCi/nmol (3.0 mCi/mg polymer) were obtained upon radiolabeling with ^{111}In for the 43, 20 and 10 kD conjugates, respectively. Following radiolabeling, net charge contributed by CHX-A"-DTPA was calculated to have changed approximately 0.05% for all conjugates, and deemed negligible.

Competitive binding of the conjugates

Prior to competitive binding assays, binding isotherm of interaction between ^{125}I -echistatin and $\alpha_v\beta_3$ integrin expressed on HUVECs was established to determine total, specific and nonspecific binding as well as concentration of radio-ligand to be used for competitive binding assays (data not shown). Competitive binding assay results demonstrate that upon incubating HPMA copolymer-RGDfK conjugates with radiolabeled echistatin the copolymers bind to the $\alpha_v\beta_3$ integrin. The decrease in percent bound ^{125}I echistatin (Figure 2) with an increase in copolymer concentration suggests both compounds compete for the same receptor. IC_{50} values (nM peptide) as determined by non-linear regression were as follows: 929 ± 1.55 , 794 ± 1.51 , 398 ± 1.38 and 513 ± 1.29 for the 43, 20 and 10 kD conjugates and free RGDfK, respectively. At equivalent peptide concentrations, highest apparent binding affinity was observed for the 10kD conjugate.

Biodistribution of HPMA copolymer-RGDfK conjugates

Time dependent biodistribution of radiolabeled polymer-peptide conjugates was evaluated by scintigraphy and whole organ necropsy of syngeneic mice bearing Lewis lung carcinoma tumors. Figure 3 shows representative images taken at 1, 24, 48 and 96 h p.i.. Qualitative assessment of the images indicates rapid decrease in blood pool activity and distribution into organs at 1 h. Images for the 43 and 20 kD conjugates clearly indicate bladder activity at 1 h with sustained kidney activity for remaining time points, while images for the 10 kD conjugate show mainly bladder activity. The images do not show activity in the tumor above background for any of the conjugates.

The results of a 10-day biodistribution study for each copolymer molecular weight (Figure 4) demonstrated that rapid blood clearance was observed for all molecular weights with a near loss of activity after 1 hour. No significant differences in blood pool activity were observed for different molecular weights.

Copolymers accumulated in background organs to a larger extent with little tumor accumulation. Kidney, liver and spleen had significant accumulation ($p < 0.001$) over tumor for each copolymer studied. Tumor accumulation for all copolymers was insignificant compared to major organs. There were no significant differences in tumor accumulation between the polymers of different molecular weight.

Highest organ activity was observed in the kidneys for all conjugates, having enhanced accumulation over all organs for each M_w ($p < 0.001$). Additionally, significant differences were observed for kidney accumulation between molecular weights, indicating a molecular weight dependence on renal elimination. For the 43 and 20 kD conjugates, peak kidney accumulation occurred at 6 h, followed by slow elimination. The 10 kD conjugate freely passed through the kidney, with max activity occurring at 15 min. A molecular weight effect was also observed

on liver and spleen accumulation for the larger 43 kD conjugate having significant ($p < 0.001$) accumulation over the 20 and 10 kD conjugates.

To verify that copolymers primarily eliminated through the kidney, urine was collected and radioactivity measured from groups of 4 animals for each conjugate (Figure 5). Differences in cumulative urinary excretion were observed for the copolymers. The extent of renal elimination clearly shows an inverse molecular weight dependence on excretion. The 10 kD conjugate showed the highest urinary excretion, approximately 57 %ID after 3 days. Urinary excretion of the 43 and 20 kD conjugates was approximately 24 and 45 %ID, respectively.

Area-under-the-curve (AUC) pharmacokinetic analyses were performed on select organs to compare organ exposure between copolymers in the current study with that of previously studied 35 kD copolymer with 5 mol% feed of CHX-A"-DTPA [7]. Dose normalized AUC values as determined by trapezoidal integration from 0 to 240 h (Table 2) show high exposure to the liver, spleen and kidney while low exposures for the blood and tumor. Highest organ exposure was observed for the 43 kD conjugate, except tumor which showed very similar accumulation between the 43 and 20 kD conjugates.

DISCUSSION

This study evaluated the effects of increased electronegative charge and varying molecular weight of targetable HPMA copolymer-RGDfK conjugates on in vitro binding to HUVEC cells and in vivo biodistribution in tumor-bearing mice. Previously we demonstrated that cyclic RGD peptides attached to HPMA copolymers have bioadhesive properties to HUVEC cells and enhanced accumulation in solid tumors in vivo [5–7]. We further demonstrated that such copolymers containing therapeutic radionuclides significantly arrest tumor growth in murine models of prostate cancer [8]. An unresolved issue in targeting radiotherapeutics to solid tumors by systemic administration is radiotoxicity to non-target organs. To minimize their toxic effects, we synthesized HPMA copolymer-RGDfK conjugates with varying molecular weight and charge content in an attempt to identify a structure that maximizes tumor accumulation while rapidly clearing other organs. Polymerization and subsequent size fractionation of polymers from the same batch was necessary to control comonomer incorporation between copolymers of different molecular weights. The physicochemical characteristics of the copolymers show similar content of comonomers per gram of polymer between the fractions. The approximate number of moieties per polymer backbone decreased correspondingly with decreased copolymer molecular weight. CHX-A"-DTPA in the polymer backbone was used as a stable chelating agent for radioactive isotopes [21] and to impart a high level of negative charge at relatively little expense to monomer feed ratio due to the five carboxylic acid residues per chelator in the side chains. Attaining a negatively charged backbone with such a molecule leaves room in the feed mixture to increase the content of targeting moiety, additional comonomers, or the HPMA comonomer in order to keep the polymers water-soluble and targetable.

Prior to in vivo study, copolymers were tested in vitro to verify that RGDfK peptides attached to copolymer side chains retained binding activity. In the past we have used an endothelial cell adhesion assay to assess targetability to the $\alpha_v\beta_3$ integrin. In this study we used a radiolabeled competitive binding assay that generated binding affinity values. These studies showed that peptides attached to polymeric backbones remained active and bound to the $\alpha_v\beta_3$ integrin. The increase in charge did not affect binding affinity in vitro. A decrease in binding affinity per peptide with an increase in polymer M_w suggests that smaller polymer chains provide more peptides accessible to the receptors due to decreased steric hindrance.

The gamma emitting ^{111}In radionuclide was chosen to radiolabel the conjugates for biodistribution studies due to its clinical acceptability, relatively long half life for imaging and chelation stability to CHXA"-DTPA [20]. While in vitro data showed active targeting to endothelial cells, interestingly once administered in vivo the extent of tumor accumulation of the highly charged polymers was minimal. This is despite our previous observation that HPMA copolymer-RGDfK conjugates with 5 mol% feed of CHX-A"-DTPA had enhanced tumor accumulation relative to non-targeted systems. The influence of increased electronegativity of HPMA copolymers was first observed as rapid blood clearance. Nearly the entire dose cleared from the blood after 1 h. It is clear from these findings that controlling blood clearance is important for tumor accumulation. Partitioning from blood to tumor through passive and active targeting mechanisms requires time, and accumulation can be reduced if residence time in blood is short.

Significantly increased kidney activity over time was observed for larger M_w conjugates with a rapid decrease in blood pool activity. Our findings suggest that the polymers studied here enter the kidney and are filtered into the urine to a certain extent, but those that do not filter do not return to circulation, remaining entrapped in the kidney. Highest recovery of the conjugates in urine occurs within 24 h, with modest increases out to 72 h (Figure 5). Radioactivity recovered in urine beyond 24 h is far less than what was measured in the kidney, additionally suggesting prolonged accumulation. The accumulation of the copolymers in kidney in turn with the rate of kidney perfusion is the main reason for a rapid decrease in the observed blood accumulation for the copolymers. Interestingly, the effect was primarily observed for the 43 and 20 kD conjugates, as the 10 kD conjugate showed a decrease in kidney accumulation from the start of the experiment. However, accumulation for the 10 kD conjugate in the kidney was still higher at 192 h (3.4% ID/g) compared to a previously studied 35 kD copolymer containing 5 mol% CHX-A"-DTPA (0.6% ID/g) [7].

Although the potential exists under certain disease conditions for RGD-mediated interactions in the kidney to cause increased accumulation [22], this does not seem to be an important factor in our studies because enhanced kidney accumulation was never observed for any other previously studied HPMA copolymer-RGD conjugates [5–7]. Our previous data in fact suggests that attachment of RGD-based peptides to HPMA copolymers reduces accumulation in the kidney [5]. Also intriguing from these findings is that all copolymer conjugates studied were below the renal threshold value (approximately 45 kD) for HPMA copolymers [12].

Calculating AUC values for our radioisotope-bearing copolymers allows estimation of the radioactive exposure of a particular organ and analysis of variations in organ exposure between different types of polymers studied. In this study, organ exposure was the highest in the kidney for each conjugate, and a decrease in exposure occurred with lower M_w conjugates. AUC data presented in our previous studies allows us to compare the effect of increased CHX-A"-DTPA content on organ accumulation for the copolymers. We previously reported AUC values for a 35 kD HPMA copolymer-RGDfK conjugate containing 5 mol% CHX-A"-DTPA feed ratio and administered with an average dose of 265 μCi (Table 2). This polymer conjugate had increased blood circulation time represented by an increase in blood AUC value of 989.1 $\mu\text{Ci/g.h}$ as compared to 42.6 $\mu\text{Ci/g.h}$ for the 43 kD conjugate studied here (See Table 2). Tumor accumulation was also drastically altered. The previous 35 kD copolymer conjugate had a tumor AUC value of 4424.9 $\mu\text{Ci/g.h}$ as compared to 222.2 $\mu\text{Ci/g.h}$ for the 43 kD conjugate studied here, nearly 5% of exposure as previously reported. These results suggest that by increasing CHX-A"-DTPA content, tumor and blood pool concentrations decrease, even when comparing a copolymer of higher M_w . However, it should be clarified that apart from differences in the conjugate molecular weight and CHX-A"-DTPA content between these two studies, there are also differences in the RGDfK content (12 peptides [7] vs 9 peptides for 43 kD conjugate in the current study). This slight variation in polymer architecture may affect the

globular structure (hydrodynamic volume and radius) of these copolymer conjugates causing slightly different in vivo biodistribution, however it is unlikely that these small changes would account for the current observations attributed to increasing the CHX-A"-DTPA content.

Recently, the in vivo biodistribution in mice of a bone-targeting HPMA copolymer containing Daspartic acid octapeptide as a targeting moiety was reported [23,24]. These copolymers contained similar electronegative charge content as copolymers reported in our study due to the multiplicity of carboxylic acid functional groups in the aspartic acid-based targeting moiety. Significant kidney clearance of the copolymers with highest accumulation for a 96 kD conjugate near 2% ID/g at 24 h was observed. At this point the reason for the observed accumulation of the CHX-A"-DTPA containing copolymer is unknown to us. Nevertheless, the data clearly shows that incorporation of increased amounts of CHX-A"-DTPA overcomes the predicted effect of the RGDfK targeting moiety in vivo.

Renal drug targeting is an area of growing importance for treatment of kidney disease and has been recently reviewed by Dolman, et al [25]. Previous investigations into carriers which target the renal system have shown that anionized polyvinylpyrrolidone (PVP) copolymers selectively accumulate in kidneys versus neutral and cationized PVP copolymers [26,27]. Eighty percent of poly(vinylpyrrolidone-co-dimethyl maleic anhydride) copolymers accumulated in kidneys at 24 h p.i. with 40% of the dose remaining in kidneys at 96 h [27]. By comparison, approximately 40% of the 43 kD HPMA copolymer studied here accumulates in kidneys at 24 h, with approximately 34% remaining in the kidney after 96 h (data not shown). The extent of kidney accumulation of the HPMA copolymers studied here is intriguing. It is important to determine whether this occurs through passive or active mechanisms. As a whole, we speculate that these polymers are taken up in the proximal tubules with slow kidney clearance as shown for other polymer-based macromolecules [26,27], however this requires further in vitro and in vivo investigations to confirm. Interesting to note is the finding that the extent of carboxylation of anionic copolymers effects kidney accumulation. Also, the type of negative charge plays an important role shown by lower renal accumulation of sulfonated PVPs [26]. This suggests that for a particular copolymer system, there may be an optimal amount of carboxylic acid residues required for higher kidney accumulation. This may explain to an extent why we see differences in kidney accumulation as compared to previous studies with lower carboxylic acid content in HPMA copolymer side chains [7].

Based on in vitro competitive binding assays, all three polymers studied are bioactive towards the $\alpha_v\beta_3$ integrin, and show a trend of increased binding affinity with a decrease in molecular weight. However, despite copolymer conjugates being biorecognizable in vitro, in vivo tumor targeting has been over-influenced by other dynamics in an in vivo system such as high kidney accumulation and rapid blood clearance. This study highlights the requirement of blood pool residence for tumor accumulation. Further evaluation of alternative polymer designs with changes in molecular weight and CHX-A"-DTPA content is necessary to minimize kidney and maximize tumor accumulation, reducing nonspecific toxicity of an active radiotherapeutic to the greatest extent. In addition, the mechanism of kidney accumulation of the copolymers studied merits further investigation.

CONCLUSION

Tumor accumulation of targetable HPMA copolymer-RGDfK conjugates is highly sensitive to blood pool residence time. In vivo, HPMA copolymers bearing increased amounts of CHX-A"-DTPA resulted in preferential kidney accumulation, causing rapid blood pool clearance and an absence of significant tumor accumulation. Comonomer feed ratios of tumor-targeted copolymers must be carefully balanced in order to maintain low non-specific uptake with high

tumor localization. The mechanism of kidney accumulation of CHX-A"-DTPA-containing HEMA copolymers requires further investigation.

ACKNOWLEDGEMENTS

The authors would like to thank Kristin Lanham and Jennifer Lahner for imaging experiments and Omer Aras for biodistribution studies. Authors are also grateful for insightful manuscript input from Jindrich Kopecek and Amitava Mitra. This research was supported by American Russian Cancer Alliance, National Institutes of Health grant R01 EB007171 and by Department of Defense Multidisciplinary Postdoctoral Fellowship W81XWH-06-1-0698 to RK. MB is in part supported by an American Foundation for Pharmaceutical Education predoctoral fellowship and a University of Maryland Department of Pharmaceutical Sciences predoctoral fellowship.

REFERENCES

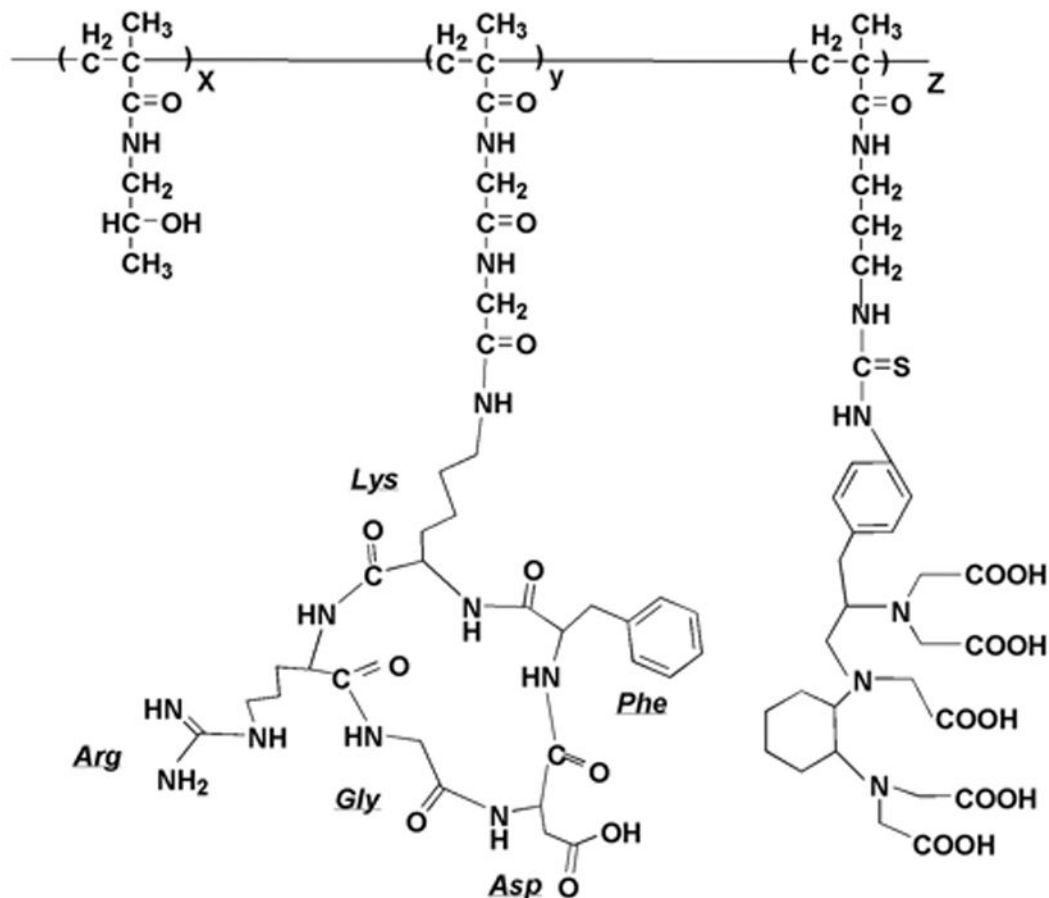
1. Kassis AI, Adelstein SJ. Radiobiologic principles in radionuclide therapy. *J. Nucl. Med* 2005;46:4–12. Scopus
2. Jin H, Varner J. Integrins: roles in cancer development and as treatment targets. *Br. J. Cancer* 2004;90(3):561–565. [PubMed: 14760364] Scopus
3. Cooper CR, Chay CH, Pienta KJ. The role of alpha(v)beta(3) in prostate cancer progression. *Neoplasia* 2002;4(3):191–194. [PubMed: 11988838]
4. Neri D, Bicknell R. Tumour vascular targeting. *Nat. Rev. Cancer* 2005;5(6):436–446. [PubMed: 15928674]
5. Line BR, Mitra A, Nan A, Ghandehari H. Targeting tumor angiogenesis: comparison of peptide and polymer-peptide conjugates. *J Nucl Med* 2005;46(9):1552–1560. [PubMed: 16157540] Scopus
6. Mitra A, Mulholland J, Nan A, McNeill E, Ghandehari H, Line BR. Targeting tumor angiogenic vasculature using polymer-RGD conjugates. *J Control Release* 2005;102(1):191–201. [PubMed: 15653145] Scopus
7. Mitra A, Coleman T, Borgman M, Nan A, Ghandehari H, Line BR. Polymeric conjugates of mono- and bi-cyclic alphavbeta3 binding peptides for tumor targeting. *J Control Release* 2006;114(2):175–183. [PubMed: 16889865] Scopus
8. Mitra A, Nan A, Papadimitriou JC, Ghandehari H, Line BR. Polymer-peptide conjugates for angiogenesis targeted tumor radiotherapy. *Nucl Med Biol* 2006;33(1):43–52. [PubMed: 16459258] Scopus
9. DeNardo SJ, DeNardo GL. Targeted radionuclide therapy for solid tumors: an overview. *Int J Radiat Oncol Biol Phys* 2006;66(2 Suppl):S89–S95. [PubMed: 16979448] Scopus
10. Lammers T, Kuhnlein R, Kissel M, Subr V, Etrych T, Pola R, Pechar M, Ulbrich K, Storm G, Huber P, Peschke P. Effect of physicochemical modification on the biodistribution and tumor accumulation of HEMA copolymers. *J Control Release* 2005;110(1):103–118. [PubMed: 16274831] Scopus
11. Mitra A, Nan A, Ghandehari H, McNeill E, Mulholland J, Line BR. Technetium-99m-labeled N-(2-hydroxypropyl) methacrylamide copolymers: synthesis, characterization, and in vivo biodistribution. *Pharm Res* 2004;21(7):1153–1159. [PubMed: 15290854]
12. Seymour LW, Duncan R, Strohalm J, Kopecek J. Effect of molecular weight (M_w) of N-(2-hydroxypropyl) methacrylamide copolymers on body distribution and rate of excretion after subcutaneous, intraperitoneal, and intravenous administration to rats. *J Biomed Mater Res* 1987;21(11):1341–1358. [PubMed: 3680316] Scopus
13. Seymour LW, Miyamoto Y, Maeda H, Brereton M, Strohalm J, Ulbrich K, Duncan R. Influence of molecular weight on passive tumour accumulation of a soluble macromolecular drug carrier. *Eur J Cancer* 1995;31A(5):766–770. [PubMed: 7640051] Scopus
14. Strohalm J, Kopecek J. Poly N-(2-hydroxypropyl) methacrylamide: 4. Heterogenous polymerization. *Angew. Makromol. Chem* 1978;70:109–118.
15. Rejmanova P, Labsky J, Kopecek J. Aminolyses of monomeric and polymeric p-nitrophenyl esters of methacryloylated amino acids. *Makromol. Chem* 1977;178:2159–2168.
16. Lu ZR, Kopeckova P, Wu Z, Kopecek J. Functionalized semitelechelic poly[N-(2-hydroxypropyl) methacrylamide] for protein modification. *Bioconj Chem* 1998;9(6):793–804. [PubMed: 9815174]

17. Rhim JS, Tsai WP, Chen ZQ, Chen Z, Van Waes C, Burger AM, Lautenberger JA. A human vascular endothelial cell model to study angiogenesis and tumorigenesis. *Carcinogenesis* 1998;19(4):673–681. [PubMed: 9600354]Scopus
18. Wu Y, Zhang X, Xiong Z, Cheng Z, Fisher DR, Liu S, Gambhir SS, Chen X. microPET imaging of glioma integrin $\{\alpha\}\nu\{\beta\}3$ expression using (64)Cu-labeled tetrameric RGD peptide. *J Nucl Med* 2005;46(10):1707–1718. [PubMed: 16204722]Scopus
19. Kumar CC, Nie H, Rogers CP, Malkowski M, Maxwell E, Catino JJ, Armstrong L. Biochemical characterization of the binding of echistatin to integrin $\alpha\nu\beta3$ receptor. *J Pharmacol Exp Ther* 1997;283(2):843–853. [PubMed: 9353406]Scopus
20. Camera L, Kinuya S, Pai LH, Garmestani K, Brechbiel MW, Gansow OA, Paik CH, Pastan I, Carrasquillo JA. Preclinical evaluation of ^{111}In -labeled B3 monoclonal antibody: biodistribution and imaging studies in nude mice bearing human epidermoid carcinoma xenografts. *Cancer Res* 1993;53(12):2834–2839. [PubMed: 8504427]Scopus
21. Camera L, Kinuya S, Garmestani K, Wu C, Brechbiel MW, Pai LH, McMurry TJ, Gansow OA, Pastan I, Paik CH. Evaluation of the serum stability and in vivo biodistribution of CHX-DTPA and other ligands for yttrium labeling of monoclonal antibodies. *J. Nucl. Med* 1994;35(5):882–889. [PubMed: 8176477]Scopus
22. Goligorsky MS, Noiri E, Kessler H, Romanov V. Therapeutic effect of arginine-glycine-aspartic acid peptides in acute renal injury. *Clin Exp Pharmacol Physiol* 1998;25:3–4. 276–279.Scopus
23. Wang D, Miller SC, Shlyakhtenko LS, Portillo AM, Liu XM, Papangkorn K, Kopeckova P, Lyubchenko Y, Higuchi WI, Kopecek J. Osteotropic peptide that differentiates functional domains of the skeleton. *Bioconjug. Chem* 2007;18(5):1375–1378. [PubMed: 17705416]Scopus
24. Wang D, Sima M, Mosley RL, Davda JP, Tietze N, Miller SC, Gwilt PR, Kopeckova P, Kopecek J. Pharmacokinetic and biodistribution studies of a bone-targeting drug delivery system based on N-(2-hydroxypropyl)methacrylamide copolymers. *Mol. Pharm* 2006;3(6):717–725. [PubMed: 17140259]Scopus
25. Dolman, M.; Fretz, M.; Segers, G.; Lacombe, M.; Prakash, J.; Storm, G.; Hennink, W.; Kok, R. Renal targeting of kinase inhibitors. *International Journal of Pharmaceutics*. 2008. Scopus
26. Kodaira H, Tsutsumi Y, Yoshioka Y, Kamada H. The targeting of anionized polyvinylpyrrolidone to the renal system. *Biomaterials* 2004;25(18):4309–4315. [PubMed: 15046921]Scopus
27. Kamada H, Tsutsumi Y, Sato-Kamada K, Yamamoto Y, Yoshioka Y, Okamoto T, Nakagawa S, Nagata S, Mayumi T. Synthesis of a poly(vinylpyrrolidone-co-dimethyl maleic anhydride) copolymer and its application for renal drug targeting. *Nat Biotechnol* 2003;21(4):399–404. [PubMed: 12612587]Scopus

HPMA

MA-GG-RGDfK

APMA-CHX-A''-DTPA

**FIGURE 1.**

Structure of HPMA copolymer-RGDfK peptide conjugates. Copolymers contained the monocyclized RGDfK targeting moiety to target the $\alpha_v\beta_3$ integrin with the ^{111}In chelating moiety CHX-A''-DTPA containing five acetic acid residues to render a negative charge to the backbone and to radiolabel the conjugates.

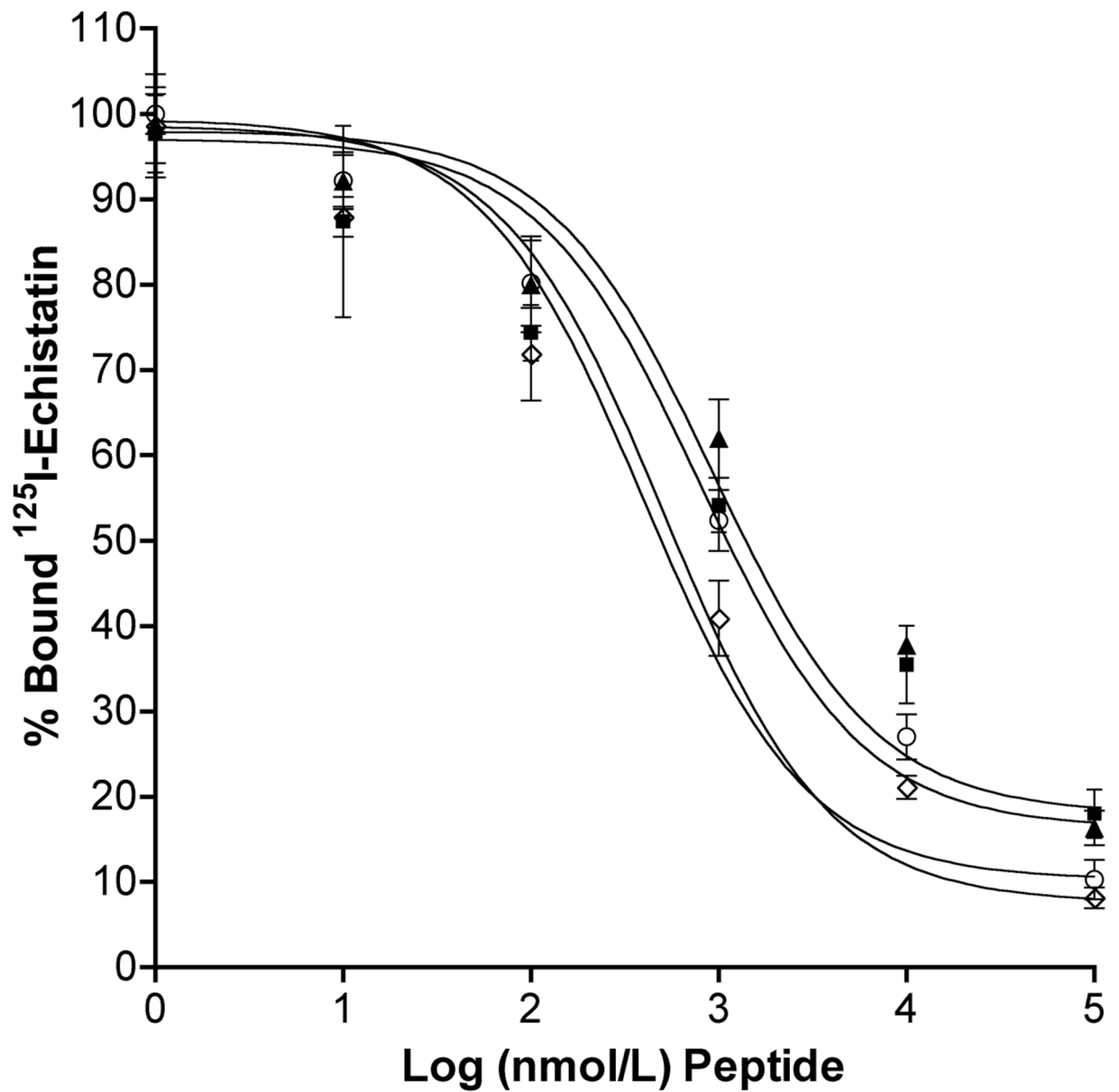
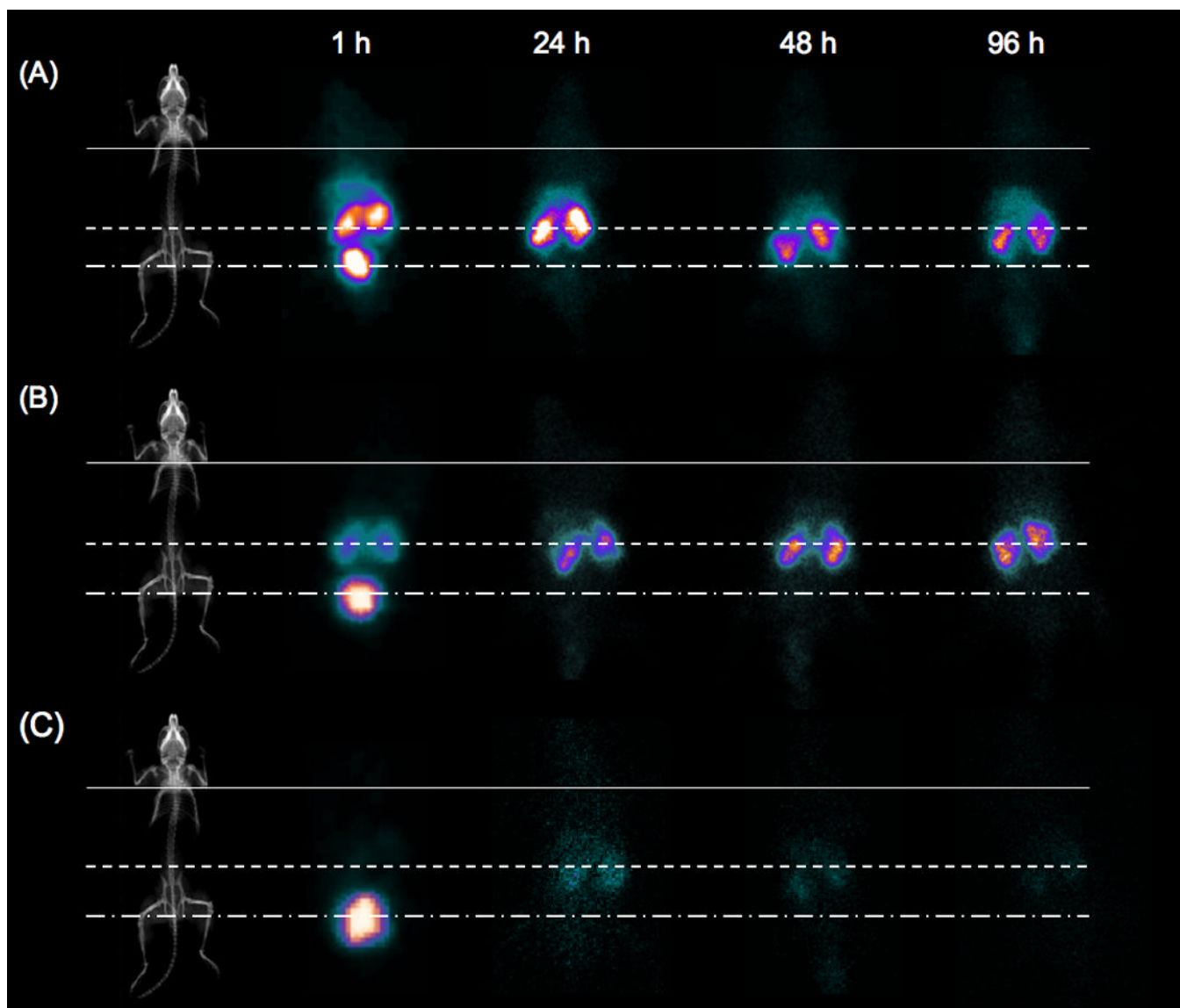


FIGURE 2. Competitive binding of HPMA copolymer-RGDfK conjugates and free peptide to HUVEC cells. Conjugates of varying M_w : 43 kD (■), 20 kD (▲), 10 kD (○) and free RGDfK (◇) inhibited binding of ¹²⁵I-echistatin to the $\alpha_v\beta_3$ integrin expressed on HUVEC cells. Results are expressed as means of triplicate \pm SD.

**FIGURE 3.**

Scintigraphic images of mice bearing Lewis lung carcinoma tumors injected with ^{111}In -labeled HPMA copolymer-RGDfK conjugates of increased electronegative charge and varying M_w . (A) 43 kD, (B) 20 kD and (C) 10 kD conjugates show no blood pool activity at 1 h and no tumor accumulation to 96 h. (A) and (B) show sustained kidney accumulation thru 96 h while (C) shows no sustained organ activity after 24 h. Lines indicate organ location: tumor (solid), kidney (dashed) and bladder (dash-dot). Images show typical animal from each time point.

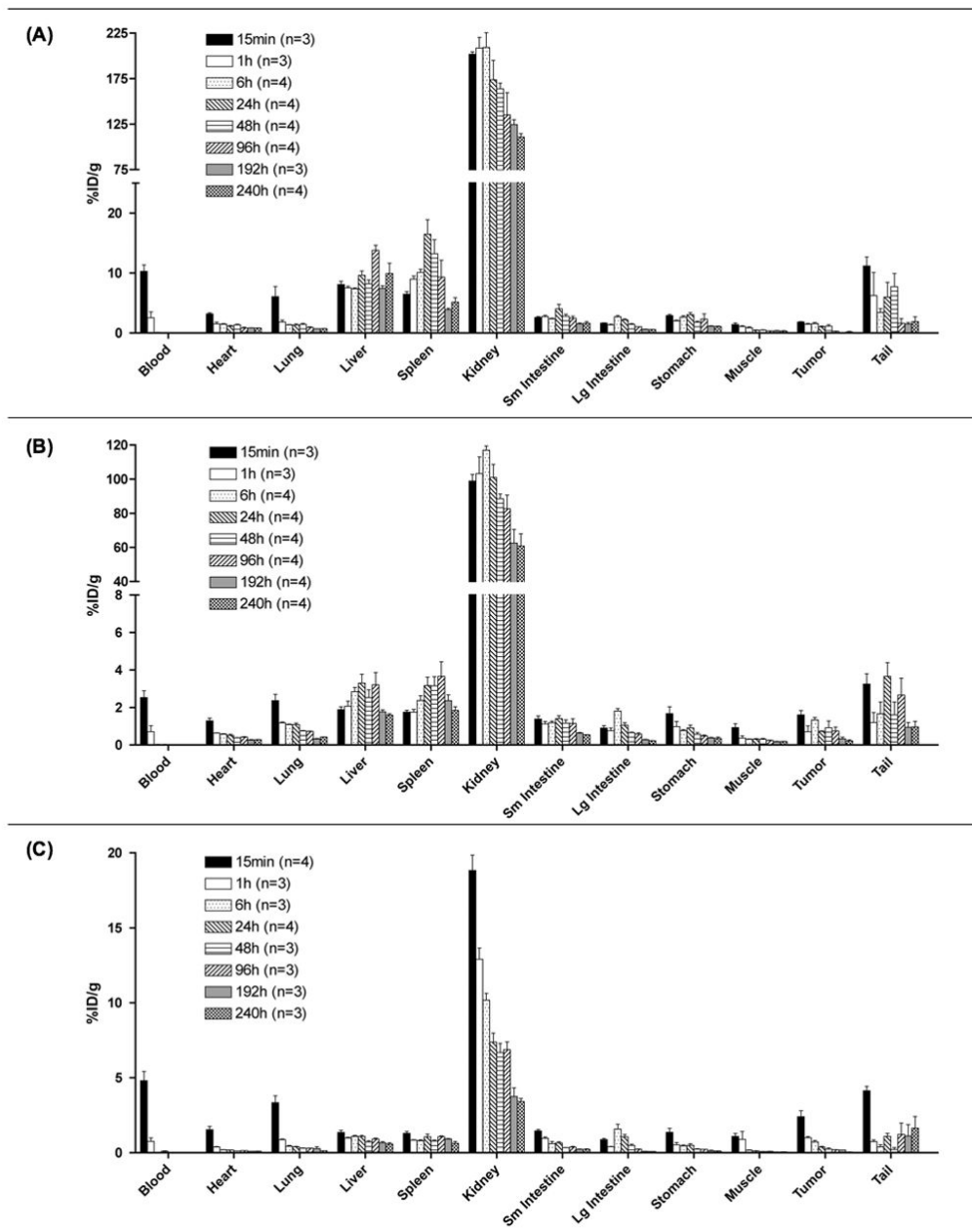


FIGURE 4. Biodistribution of ^{111}In -labeled HPMA copolymer-RGDfK conjugates with increased electronegative charge and varying M_w : (A) 43 kD, (B) 20 kD and (C) 10 kD. Activity per organ is expressed as % injected dose per gram of tissue (%ID/g) following necropsy at 15 min, 1, 6, 24, 48, 96, 192 and 240 h post-intravenous injection. Data confirms image analysis showing rapid loss of activity from blood, highest accumulation in kidney and no sustained tumor activity. Data is expressed as mean \pm SD (number of mice/group is shown).

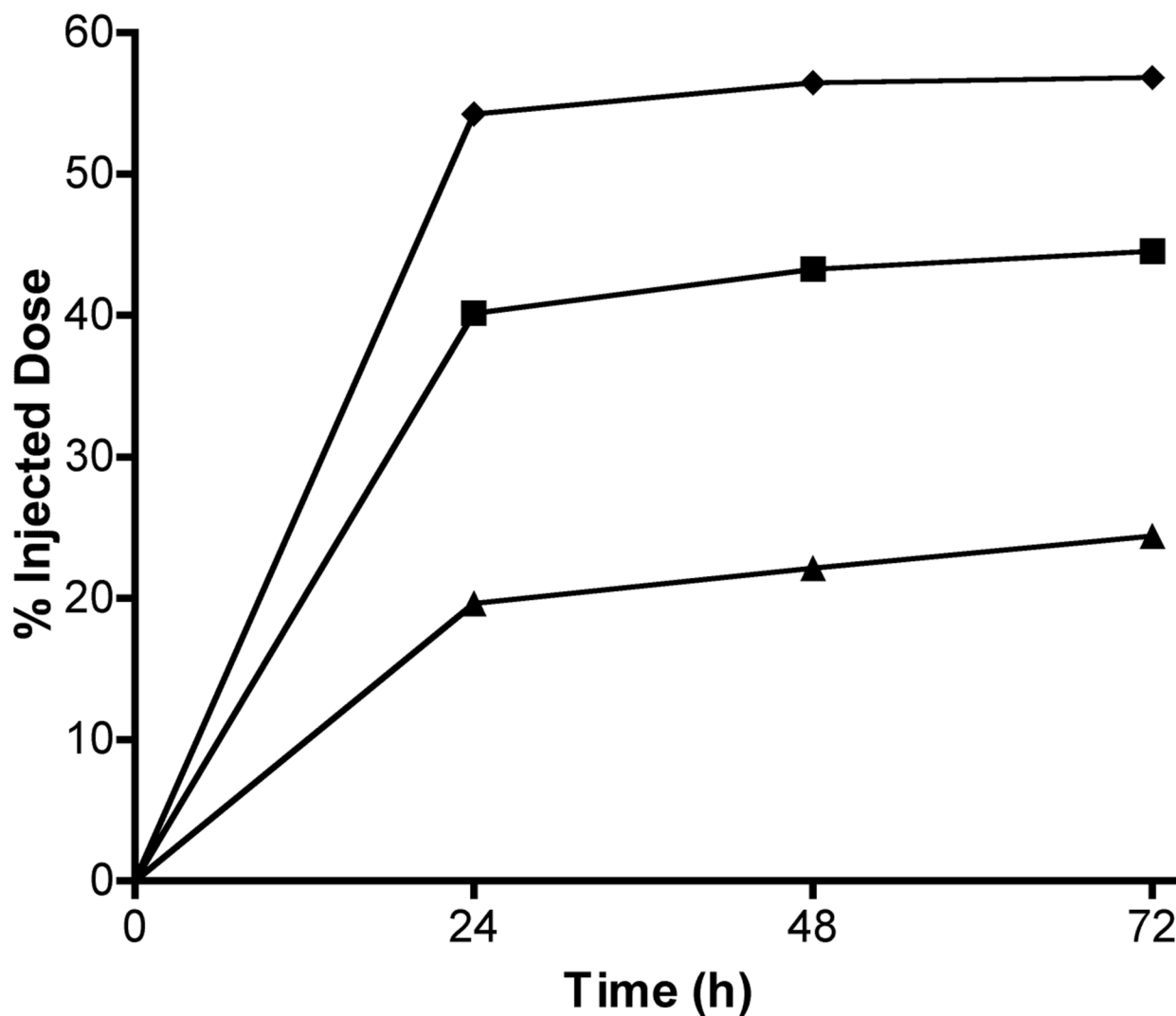


FIGURE 5.

Cumulative urinary excretion of radiolabeled copolymer conjugates. Data represents radioactivity measured in urine represented as percent injected dose recovered from groups of 4 mice per treatment injected with ^{111}In -labeled HPMA copolymer-RGDfK conjugates of varying M_w : 43 kD (▲), 20 kD (■) and 10 kD (◆). For each M_w , the largest percentage of dose was recovered in urine within 24 h. As copolymer M_w increases, a decrease in urinary excretion is observed.

TABLE 1

Physiochemical characteristics of the copolymers.

	1	2	3
Estimated M_w (kD) ^a	42.7	19.5	9.9
Polydispersity ^a	1.2	1.1	1.1
CHX-A"-DTPA content (mmol/g polymer) ^b	0.266	0.266	0.275
CHX-A"-DTPA incorporation (%) ^c	73.3	73.5	75.9
RGDfK content (mmol/g polymer) ^d	0.210	0.282	0.295
RGDfK incorporation (%) ^c	57.9	77.7	81.3

^a As determined by size exclusion chromatography^b Spectrophotometric analysis (Mean \pm SD, n = 3)^c Feed ratio^d Determined by amino acid analysis

TABLE 2
Dose normalized area under the curve (AUC) * values for ^{111}In -HPMA copolymer-RGDfK conjugates.

Polymer M_w (kD)	Dose Normalized AUC ($\mu\text{Ci/g}\cdot\text{h}$)				
	Blood	Liver	Spleen	Kidney	Tumor
43	42.6	4932.5	3685.7	72514.2	222.2
20	9.6	1146.7	1326.6	41741.8	225.5
10	12.2	376.3	455.0	2816.2	98.1
35**	989.1	957.2	739.2	1591.6	4424.9

* AUC values were calculated by using trapezoidal integration of radioactivity concentrations ($\mu\text{Ci/g}$ tissue, calculated from necropsy biodistribution data) versus time curves from 0 h to 240 h post-injection. Normalized to average dose (136.3 μCi) for 10 kD conjugate.

** For comparison 35 kD HPMA copolymer-RGDfK conjugate containing 5 mol% feed ratio of CHX-A''-DTPA as previously reported [7].